Improving mould design and injection parameters in metal injection moulding by accurate 3D finite element simulation

Thierry Barrière, Jean-Claude Gélin, Baoshung Liu

Improving mould design and injection parameters in metal injection moulding by accurate 3D finite element simulation

T. Barrière[a], J.C. Gelin[a,*], B. Liu[b]

[a]*Laboratoire Mécanique Appliquée R. Chaléat, UMR CNRS 6604, 24 rue de l'Epitaphe, 25030 Besancon Cedex, France*

[b]*Institute of Engineering Science, Southwest Jiatong University, 610031 Chengdu, Sichuan, PR China*

The metal injection moulding (MIM) process combines the well-known thermoplastic injection and powder metallurgy technologies to manufacture small and intricate parts to nearly net shape. The design of injection moulds is a very important stage in such a technology as the mixture of metallic powder and thermoplastic binder is injected in the mould with a viscous behaviour strongly different from the pure polymer injection. To improve the mould design by an efficient numerical tool, an explicit 3D software has been developed to perform efficiently the injection simulation. Taking into account the special behaviour of feedstock in MIM injection, a bi-phasic model is used to describe the flows of metallic powder and plastic binder so as to predict accurately the powder segregation in injection. The volume fractions of metallic powder and plastic binder give directly the evolution of segregation during the injection course. The numerical results are compared with experiments, in which a multi-cavity mould specially designed and realised in our laboratory is used. The segregation zones are well predicted. This specially developed software permits to optimise the mould design and processing parameters to get required components.

Keywords: Metal injection moulding; Numerical simulation; Mould design; Injection parameters

1. Introduction

Mould design and determination of the injection parameters is a key problem to realise successfully the manufacturing of parts by metal injection moulding (MIM) technology. This new manufacturing technique is expected to be very efficient way to produce small and complex metallic parts in large batches [1]. The injection stage is very important in such a manufacturing process as any defect, even invisible in green parts, will certainly be amplified in the next debinding and sintering stages. The feedstock that is injected in the mould is a compound of metallic powder and thermoplastic binder that exhibits a behaviour that is very different from the polymer materials. Viscosimetry tests should be used to identify the flow behaviour of the MIM feedstock generally using a capillary viscosimeter [2]. Other than the phenomena commonly existing in the polymer injection, the powder segregation is a special effect arising in MIM to be predicted in simulation [3,4]. This effect may happen near mould corners and sudden changes of the flow sections in the mould. However, the powder and binder possess very different mass densities and flow behaviour, resulting in the possibilities of changing their volume fractions during injection moulding. This special phenomenon makes it impossible to simulate the MIM injection stage with standard software used for polymer injection.

To remedy this imperfection, some authors suggested to employ the mixture theory for modelling the MIM injection stage [5,6]. Such an approach is proved to be convenient for the description of the liquid flows charged with powder in high concentration. It is suitable for the modelling of MIM injection but remains difficult due to tremendous computational costs for coupled bi-phasic flows, especially for 3D industrial problems. The conventional implicit methods have been proved to be feasible but make the simulation costs unrealistic for large scale problems. A new explicit method is introduced in this paper to perform efficiently the bi-phasic injection stage simulation. The prediction of segregation effects, as well as others sorts of injection defects, is then realisable in an efficient manner. This new simulation strategy leads to the improvement of mould design and injection parameters with a suitable numerical tool. The

* Corresponding author. Tel.: +33-381-666035; fax: +33-381-666700.
E-mail address: jean-claude.gelin@univ-fcomte.fr (J.C. Gelin).

numerical results are validated by comparison with experiments conducted in the laboratory.

2. The mixture theory and explicit algorithm for simulation

The mixture theory is suitable to describe the flows of viscous binder charged with particles in high concentration. The injection flow is considered as the addition of two distinct but coupled flows, which are characterised by the velocities of polymer binder and metallic powder. These two flows are named respectively fluid phase flow and solid phase flow. The coupling term between both flows is associated to their momentum exchange. Two variables respectively named the solid and fluid volume fractions ϕ_s and ϕ_f are defined to represent proportions of powder and binder in the filled portion of the mould at each instant t. It is their variation during injection moulding that represents directly the segregation effects during the MIM injection stage. The flows of solid and fluid phases possess two co-existent velocity fields V_s and V_f. The effective velocity V_{ef} or so-called mixture's velocity is then defined as:

$$V_{ef} = \phi_s V_s + \phi_f V_f \tag{1}$$

2.1. Evolution of the filling state

The evolution of filling state during the injection stage is described by a field variable F. At each instant t during injection F takes a value equal to 1 in the filled domain and a value equal to 0 for the void portion of the mould. This variable obeys an advection equation as in polymer injection but is mainly driven by the effective velocity of the mixture:

$$\frac{\partial F}{\partial t} + \nabla \cdot (V_{ef} F) = 0 \tag{2}$$

The numerical solution for the advection equation associated to the filling state uses the same scheme as in polymer injection simulation except that the velocity field is replaced by effective velocity of the mixture. For sake of the stability, a Taylor–Galerkin method is used [6,7].

2.2. Mass conservation and phase segregation

As mentioned above, two field variables ϕ_s and ϕ_f are used to describe their proportions in the filled domain. Saturation condition should be verified, such as:

$$\phi_s + \phi_f = 1 \quad \text{and} \quad \frac{\partial \phi_s}{\partial t} + \frac{\partial \phi_f}{\partial t} = 0 \tag{3}$$

The intrinsic densities of each phase remain constant ρ_{s0} and ρ_{f0}. The apparent density for each phase in the mixture is related to its volume fraction, defined by the following relations:

$$\rho_s = \phi_s \rho_{s0} \quad \text{and} \quad \rho_f = \phi_f \rho_{f0} \tag{4}$$

where ρ_s and ρ_f are respectively the apparent densities for solid and fluid phases in the mixture. Mass conservation should be verified by the flows of each phase p, $\forall p \in \{s, f\}$, so that:

$$\frac{\partial \rho_p}{\partial t} + \nabla \cdot (\rho_p V_p) = 0 \tag{5}$$

Eq. (5) coupled with the saturation condition (3) are very important for the prediction of the segregation effects during injection moulding simulation. The evolution of volume fractions for both phases is directly related to segregation. Taking into account the saturation constraint, the incompressibility condition for mixture flow should be verified:

$$\nabla \cdot V_{ef} = 0 \tag{6}$$

2.3. Momentum conservation and exchange

In the injection stage for MIM, the Reynolds number is generally very small. So the momentum conservation equations lead generally to two distinct Stokes equations [8,9]. The coupling between the flows of both is introduced by a momentum exchange term $\boldsymbol{m}_s = -\boldsymbol{m}_f$. For each phase p, $\forall p \in \{s, f\}$, one has:

$$\rho_p \frac{\partial V_p}{\partial t} = -\nabla(\phi_p P) + \nabla \cdot \sigma'_p + \rho_p g + \boldsymbol{m}_p + f_p^{ext} \tag{7}$$

where P stands for the pressure field in the mixture, σ'_p the deviatoric Cauchy stresses which take into account only the viscous effects in the same phase, and g the gravity acceleration vector:

$$\forall p \in \{s, f\}, \quad \sigma'_p = 2\mu_p(T, \phi_p, \dot{\varepsilon}'_p)\dot{\varepsilon}'_p \tag{8}$$

where μ_p represents the viscosity behaviour to be determined under the frame of mixture theory for each phase. They are function of temperature, volume fractions and effective shear rate, $\dot{\varepsilon}'_p$ stands for the deviatoric strain rates for each phase, and T indicates the temperature value.

The coupling terms between the flow of both phases are proportional to the difference of their velocities at each spatial point:

$$\boldsymbol{m}_s = k(V_f - V_s) \quad \text{and} \quad \boldsymbol{m}_f = k(V_s - V_f) \tag{9}$$

where k is an interaction coefficient. Its value has to be identified by an inverse method associated to experiments [10].

2.4. Boundary conditions

The boundary conditions should be imposed for each variable entering in the solution process. For Stokes equations, the mould inlets can have the imposed velocity or imposed pressure. The boundary conditions for solid and fluid volume fractions or filling state variable should also be

imposed on the mould inlet. The prescribed volume fractions should verify the saturation condition. On the mould outlet, one needs simply to impose a zero pressure, assigned to atmosphere pressure. For boundary conditions on the mould walls, the velocity Γ^{w} in normal direction is always imposed to zero. A tangent viscous load f should be specified for sliding conditions [11]. This tangential load is generally expressed in Chezy's form for $\forall \mathrm{p} \in \{\mathrm{s},\mathrm{f}\}$:

$$V_{\mathrm{p}} \cdot \vec{n} = 0, \quad f_{\mathrm{p}} = -c^{-2}\rho |V_{\mathrm{p}} \cdot \vec{t}| V_{\mathrm{p}} \cdot \vec{t} \tag{10}$$

where $\vec{n}$ is the unit outward normal, $\vec{t}$ the unit local tangent vector, c a coefficient to be determined by experiments. The result obtained in the void portion of the mould is not really interesting. To simplify the numerical methods, two fictitious phases are supposed in void portion of the mould. They are simply supposed to be Newtonian viscous flow with the artificial law values for their viscosities.

MINI-elements are chosen for FE modelling, as the MIM injection is modelled as a complex incompressible flow. These elements satisfy the so-called Babuska–Brezzi conditions in a global sense [12]. As the order of interpolation functions for velocity fields is higher than for pressure field, the interpolation function for velocity field is noted as N_i^+ while that for other variables is noted as N_i.

To take the important dynamic effects into account and to get the best efficiency, an explicit algorithm in fractional steps is proposed for MIM simulation. It is a complex extension of the method proposed by Lewis and co-authors [13,14] in 2D mono-phasic case. With the elements in mixed formulation, both coupled Stokes equations are solved in three fractional steps.

2.5. Phase interaction

The interaction between the flows of both phases is considered as a momentum exchange term, which is proportional to the velocity difference between both phases. Supposing that $n+1$ is the number of current time steps, one introduces a fractional step to take the interaction effect into account with the finite element discretisation expressed as:

$$\begin{aligned} \boldsymbol{M}_{\mathrm{s}}\left[\frac{V_{\mathrm{s}}^* - (V_{\mathrm{s}})^n}{\Delta t}\right] &= \boldsymbol{K}_1 \cdot (V_{\mathrm{f}} - V_{\mathrm{s}})^n, \\ \boldsymbol{M}_{\mathrm{f}}\left[\frac{V_{\mathrm{f}}^* - (V_{\mathrm{f}})^n}{\Delta t}\right] &= \boldsymbol{K}_1 \cdot (V_{\mathrm{s}} - V_{\mathrm{f}})^n \end{aligned} \tag{11}$$

where n indicates the values obtained in the last time step, V_{s}^* and V_{f}^* the intermediate values obtained in the fractional step, $\boldsymbol{M}_{\mathrm{s}}$ and $\boldsymbol{M}_{\mathrm{f}}$ the lumped mass matrices for solid and fluid phases, and $\boldsymbol{K}_1$ an interaction matrix. It is constructed numerically as:

$$\boldsymbol{K}_1 = \underset{\Omega}{A}\int_{\Omega^{\mathrm{e}}} N^{\mathrm{T}} k N \,\mathrm{d}\Omega \tag{12}$$

The symbol A represents assembling operator associated to the finite element method. As the mass matrices are lumped into diagonal forms, the solution is an explicit and uncoupled one.

2.6. Viscous diffusion

The effects of viscous diffusion in the flow of each phase are solved with another fractional time step. This solution procedure is written as:

$$\forall \mathrm{p} \in \{\mathrm{s},\mathrm{f}\}, \quad \boldsymbol{M}_{\mathrm{p}}\left(\frac{V_{\mathrm{p}}^{**} - V_{\mathrm{p}}^*}{\Delta t}\right) = \boldsymbol{K}_2(V_{\mathrm{p}}^*) + \boldsymbol{F}_{\mathrm{p}} \tag{13}$$

where V_{p}^{**} stands for another couple of intermediate values for velocity fields, $\boldsymbol{K}_2(V_{\mathrm{p}}^*)$ represents the diffusion terms for solid phase and fluid phase:

$$\forall \mathrm{p} \in \{\mathrm{s},\mathrm{f}\}, \qquad \boldsymbol{K}_2(V_{\mathrm{p}}) = \underset{\Omega}{A}\int_{\Omega^{\mathrm{e}}} (B^+)^{\mathrm{T}} \sigma'_{\mathrm{p}} \,\mathrm{d}\Omega \tag{14}$$

where B^+ is the gradient operator defined at the element level to calculate the strain rate by velocity values, σ'_{p} the deviatoric Cauchy stresses obtained by the viscous laws of each phase and $\boldsymbol{F}_{\mathrm{p}}$ the external force vectors for solid and fluid phases.

2.7. Incompressibility and pressure field

The effective velocity of mixture V_{ef} should verify the incompressibility condition (7). This condition is satisfied in a fractional step scheme as:

$$\forall \mathrm{p} \in \{\mathrm{s},\mathrm{f}\}, \quad \boldsymbol{M}_{\mathrm{p}} \frac{V_{\mathrm{p}}^{n+1} - V_{\mathrm{p}}^{**}}{\Delta t} = -\phi_{\mathrm{p}} \boldsymbol{C} P \tag{15}$$

It results that the pressure field P is solved in a global step as:

$$[\boldsymbol{C}^{\mathrm{T}} \boldsymbol{M}_{\mathrm{eq}}^{-1} \boldsymbol{C}] P = \frac{1}{\Delta t} \underset{\Omega}{A} \{\phi_{\mathrm{s}} \boldsymbol{C}^{\mathrm{T}} V_{\mathrm{s}}^{**} + \phi_{\mathrm{f}} \boldsymbol{C}^{\mathrm{T}} V_{\mathrm{f}}^{**}\} \tag{16}$$

The global operator $\boldsymbol{C}$ stands for a gradient operation, while $\boldsymbol{C}^{\mathrm{T}}$ represents a divergence one:

$$\boldsymbol{C} = A_{\Omega} \int_{\Omega^{\mathrm{e}}} [(\boldsymbol{D}^+)^{\mathrm{T}} N] \,\mathrm{d}\Omega \tag{17}$$

$\boldsymbol{D}^+$ is a divergence operator at the element level derived from N_i^+ and $\boldsymbol{M}_{\mathrm{eq}}$ an equivalent mass matrix defined as:

$$\boldsymbol{M}_{\mathrm{eq}} = \left(\frac{\phi_{\mathrm{f0}}}{\rho_{\mathrm{f0}}} + \frac{\phi_{\mathrm{s0}}}{\rho_{\mathrm{s0}}}\right)^{-1} \underset{\Omega}{A} \int_{\Omega^{\mathrm{e}}} (N^+)^{\mathrm{T}} N^+ \,\mathrm{d}\Omega \tag{18}$$

2.8. Solid and fluid phase volume fractions

Two different mass conservation equation (5) can be condensed into one when attention is paid to choose their signs, and when saturation condition is used. This let to the solution of following discretised equation:

$$\boldsymbol{M}_{\mathrm{d}} \frac{\Phi_{\mathrm{s}}^{n+1} - \Phi_{\mathrm{s}}^n}{\Delta t} = \boldsymbol{F}_{\mathrm{d}} - [\boldsymbol{K}_{\mathrm{d}}^{\mathrm{div}} + \boldsymbol{K}_{\mathrm{d}}^{\mathrm{adv}}] \Phi_{\mathrm{s}}^n \tag{19}$$

where Φ_s^n and Φ_s^{n+1} are the discretised solid volume fractions in vector form at instants t_n and t_{n+1}, respectively. The different operators in the above equation are defined as:

$$\boldsymbol{M}_d = \mathop{A}_{\Omega} \int_{\Omega^e} N^T(\rho_{s_0} + \rho_{f_0}) N \, d\Omega,$$

$$\boldsymbol{F}_d = \mathop{A}_{\Omega} \int_{\Omega^e} N^T(\rho_{f_0} \nabla \cdot V_f^e) \, d\Omega,$$

$$\boldsymbol{K}_d^{div} = \mathop{A}_{\Omega} \int_{\Omega^e} N^T[\rho_{s_0} \nabla \cdot V_s^e + \rho_{f_0} \nabla \cdot V_f^e] N \, d\Omega,$$

$$\boldsymbol{K}_d^{adv} = \mathop{A}_{\Omega} \int_{\Omega^e} N^T[\rho_{s_0} (V_s^e)^T + \rho_{f_0} (V_f^e)^T] G \, d\Omega$$

where V_s^e and V_f^e are the velocity values obtained in each elements, G a gradient operator at the element level derived from interpolation functions N_i. The solution can be performed locally as the mass matrix, $\boldsymbol{M}_d$ is lumped into a diagonal one. As the saturation condition is automatically satisfied, it becomes straightforward to predict the segregation in MIM simulation.

3. Improving mould design and injection parameters by FE simulation

3.1. Validation

The first example is aimed to validate the simulation procedure. It has been proposed by Dutilly [8]. The problem consists of a mixture flow between two parallel plates. The phase volume fractions are taken into account using the bi-phasic model with an interaction term between the flows of both distinct phases. Analytical solution is given in quasi-static formulation [8]. 2D and 3D simulations are performed using the proposed finite element software. The comparison in pressure fields has to verify the correctness and accuracy of the simulation results. The geometrical and material parameters, as well as the injection conditions, are shown in Fig. 1.

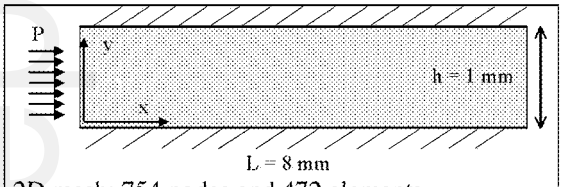

2D mesh: 754 nodes and 472 elements
3D mesh: 1247 nodes and 1247 elements

Imposed pressure: 96 MPa
Initial solid volume fraction: 50%
Interaction term: 2.10^{10} Pa.s.m^{-2}
Sticking boundary conditions on mould walls

	Solid phase	Fluid phase
Density:	7500 kg.m^{-3}	1000 kg.m^{-3}
Viscosity:	20 Pa.s	2 Pa.s

Fig. 1. Mesh, material and injection parameters for the flow between two parallel plates.

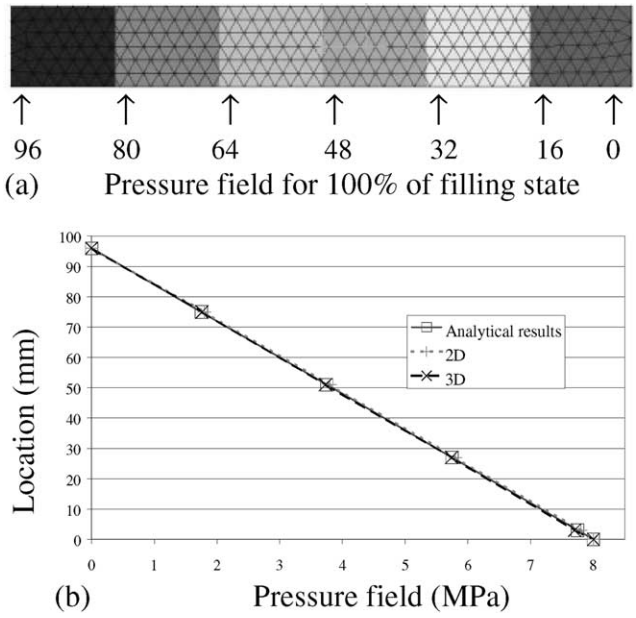

Fig. 2. (a) Pressure field obtained from 2D and 3D simulations; (b) comparison of pressure fields between simulations and analytical solution.

The results obtained by the finite element method in 2D and 3D cases, especially for pressure fields are compared to the analytical solution as shown in Fig. 2(a) and (b). According to the analytical model, the pressure should vary linearly from 96 MPa on mould inlet to 0 on mould outlet. As observed in Fig. 2, the pressure fields obtained from numerical solution correspond accurately to the analytic ones. The very slight difference is caused by the finite element discretisation.

3.2. A 3D mould cavity

The main advantage of the new algorithm for bi-phasic simulation resides on its high performance for 3D problems in large scale. It is the strongest requirement for industrial applications. To demonstrate it, the injection of a 3D bulk part has been studied, Fig. 3. This problem has been proposed in [15].

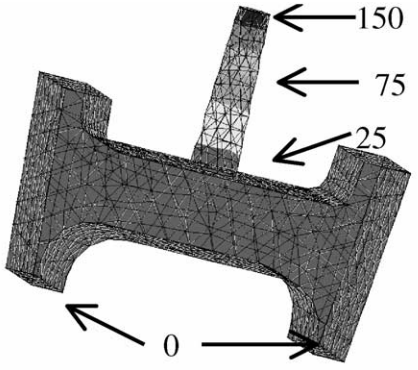

3D MINI-elements: 6297 nodes, 5045 elements

Fig. 3. Pressure contours at the end of mould filling.

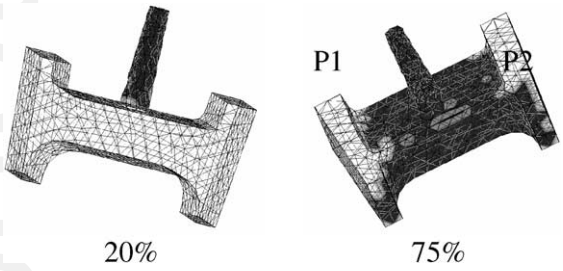

Fig. 4. Filling states corresponding to 20 and 75% of mould cavity.

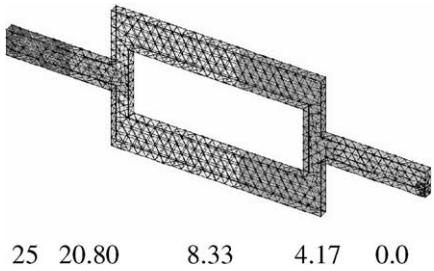

Fig. 6. Pressure field corresponding to a completely filled mould.

The bi-phasic simulation has been carried out with an imposed pressure 150 MPa on mould inlet. Sticking conditions are applied on the mould walls. The pressure contours at the end of the filling stage (Fig. 3) show that the pressure is approximately constant in the mould cavity.

Fig. 4 shows the evolution of filling front during the filling stage, corresponding respectively to 20 and 75% of mould filling. In injection course, the filling front progresses continuously until arriving to the mould outlet. The knowledge of filling patterns is one of the main goals that can be achieved by simulation. In this example, one can be aware that two lateral reinforcements P1 and P2 are not yet filled until 75% of total volume is filled, meanwhile the filling fronts have already arrived to the mould outlet. The simulation of such an example shows well the high performance of proposed algorithm for bi-phasic simulation and its potential in industrial application.

3.3. 3D simulation of a divergent–convergent mould cavity

The simulation of a 3D divergent–convergent mould cavity permits the investigation on complex flows and the validation of software performances for injection of 3D complex parts. The mould geometry, material parameters and injection conditions are given in Fig. 5.

The pressure field in the mould is shown in Fig. 6, the obtained values are symmetrical for both channels and correspond well to the decreasing pressure from the mould inlet to a zero value.

The filling fronts corresponding to four different filling ratios are shown in Fig. 7. Due to the symmetry of the mould cavity, these filling states are perfectly symmetrical as expected.

Imposed pressure: 25 MPa Initial solid volume fraction: 50% Interaction term: 10^9 Pa.s.m^{-2} Sliding without friction boundary on mould walls		
	Solid phase	Fluid phase
Density:	7500 kg.m^{-3}	1000 kg.m^{-3}
Viscosity:	20 Pa.s	2 Pa.s

Fig. 5. Mesh, material and injection parameters used for 3D simulations.

3.4. Comparisons between simulations and experiments for a four-cavity mould

The improvement of mould design and injection parameters by simulation is conducted with the experiments simultaneously carried out in the laboratory. A five-cavity mould has been specially designed and manufactured for this purpose. The simulations and experiments are performed with the same conditions to verify the design for mould cavities and the choice of injection parameters. To verify the mould design for injection, the interrupted experiments have been carried out with filling interruption at different instants to obtain the transient filling states, that permit the verification of predicted filling states. The four-cavity mould has been specially designed for that. The results corresponding to 40 and 60% for filled mould cavities are shown in Fig. 8. An excellent agreement between the numerical results and the experimental ones is observed. These comparisons attest well the effectiveness of the developed FE simulation software for MIM.

The segregation effects can also be predicted effectively. To make a precise analysis and comparison, the case corresponding to the injection of two tensile test specimens with the previous mould is chosen as an example. These two cavities make tensile test specimens to be injected by a single inlet or by two opposite ones. It makes feasible to investigate the influence of front welding on homogeneity of the green parts, and on quality of the final parts. As in the

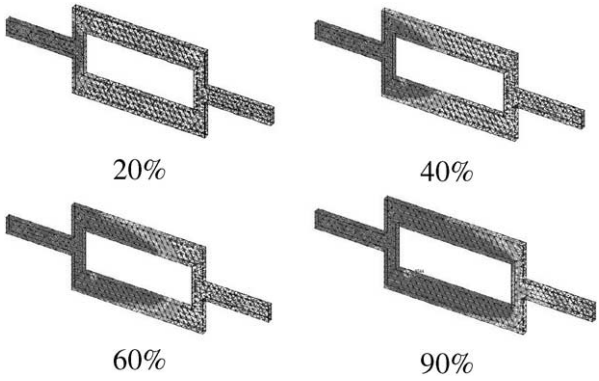

Fig. 7. Front positions corresponding to different values for mould filling (20, 40, 60 and 90%).

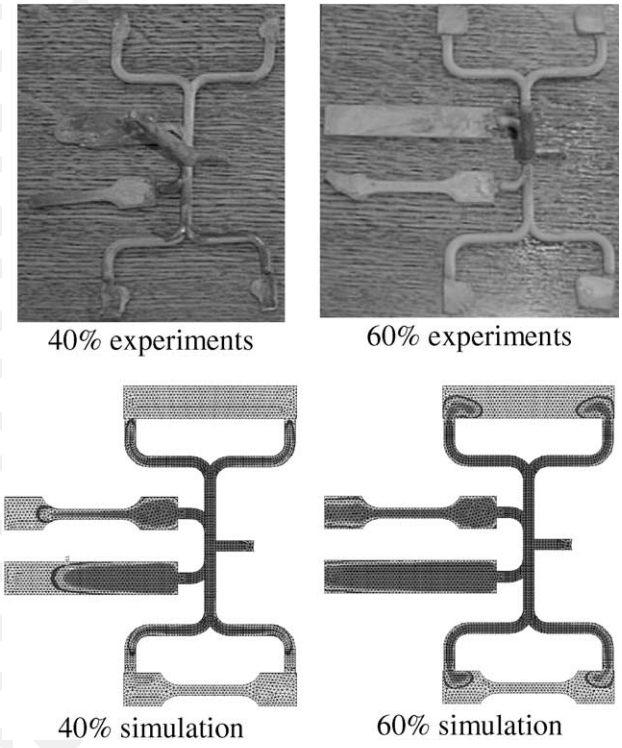

Fig. 8. Illustration of front positions corresponding to different filled stages (40 and 60%) obtained from experiments and simulation.

experimental case, the injection simulations are performed with the material behaviour corresponding to 316L thermal debinding feedstock and similar boundary conditions, Fig. 9.

The simulation results show approximately the same values for powder volume fraction in the middle of the specimens, either injected by single or two opposite ones. One obtains a value equal to 0.535 in middle of the part injected by one inlet and the part injected by two opposite inlets, a value slightly more than 0.538 is observed at the same position, see Fig. 10.

As the final mechanical properties obtained in tensile tests depend on the powder volume fraction at middle of the injected part, it results that the homogeneity in the injected

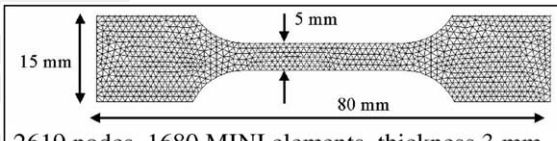

2619 nodes, 1680 MINI elements, thickness 3 mm

316L stainless steel feed stock
Injection pressure: 16 MPa
Initial powder volume fraction: 55%
Interaction term: 2.10^{10} Pa.s.m^{-2}
Sticking wall condition for two phases

	Powder phase	Fluid phase
Density	7500 kg.m^{-3}	1000 kg.m^{-3}
Viscosity	10 Pa.s	1 Pa.s

Fig. 9. Mesh for tensile test specimens.

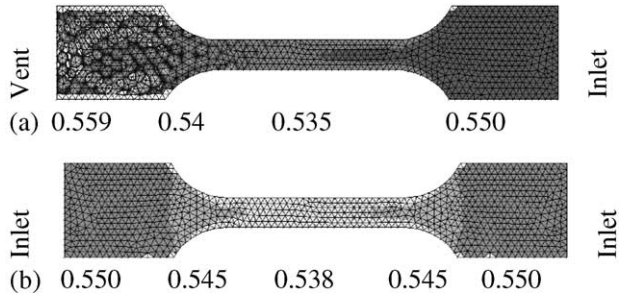

Fig. 10. Powder volume fractions in tensile specimen parts: (a) injected by single inlet; (b) injected by two opposite inlets.

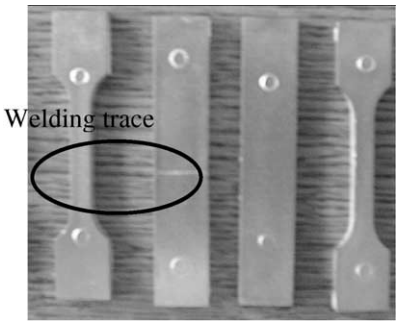

Fig. 11. Final parts after sintering.

part is a very important criterion. Tensile tests for mechanical properties on the final parts show that both types possess almost the same properties after sintering [4,6], that proves well the simulation results. The final parts after sintering for two injection patterns are shown in Fig. 11.

The only difference between different parts is a slight trace in middle of the specimen injected by two ends, which represents the front welding line in injection.

4. Conclusions

The prediction of powder segregation in MIM is necessary for an accurate simulation tool. For such a purpose, a new explicit algorithm based on the bi-phasic mixture theory has been proposed and developed to solve this strongly coupled problem in large scale. The different physical effects are evaluated in a sequential manner without any iterations. Incompressibility of the mixture is maintained by a special scheme.

The multi-cavity mould designed and manufactured in the lab has permitted the validation and improvement of mould design and parameter values for the injection stage. It proves well that the modelling of MIM injection stage by a bi-phasic model is a correct and realistic model, and that the explicit algorithm for such a model is very efficient to achieve the good results on segregation, filling state, as well as the velocity and pressure fields. The developed tool is helpful for design of the moulds for MIM.

Acknowledgements

The present program has been supported by an Invited Professor position in France, by the French–Chinese Advanced Research Program and the Backbone Professor Program of the Chinese Ministry of Education.

References

[1] R.M. German, A. Bose, Injection Molding of Metals and Ceramics, Princeton University Press, Princeton, NJ, 1997.

[2] O. Osorio, Using capillary tests to obtain viscosity data for MIM materials, in: EPMA (Ed.), Proceedings of the Second European Symposium on Powder Injection Molding, EuroPm 2000, pp. 189–195.

[3] M. Dutilly, O. Ghouati, J.C. Gelin, Finite element analysis of the debinding and densification in the process of metal injection molding, J. Mater. Process. Technol. 93 (1998) 170–175.

[4] T. Barriere, J.C. Gelin, B. Liu, Experimental and numerical investigations on the properties and quality of parts produced by MIM, Powd. Metallurgy 44 (3) (2001) 228–234.

[5] J.C. Gelin, T. Barriere, M. Dutilly, Experiments and computational modelling of metal injection molding for forming small parts, Ann. CIRP 48 (1) (1999) 179–182.

[6] T. Barriere, Expérimentations, modélisation et simulation numérique du moulage par injection de poudres métalliques, Ph.D. Thesis, University of Franche-Comté, Décembre 2000, pp. 1–219.

[7] T. Barriere, J.C. Gelin, B. Liu, Analysis of phase segregation effects arising in fluid-particle flows during metal injection molding, Int. J. Forming Process, 2002.

[8] M. Dutilly, Modélisation du moulage par injection de poudres métalliques, Ph.D. Thesis, University of Franche-Comté, 1998.

[9] B. Lanteri, H. Burlet, A. Poitou, I. Campion, Powder injection molding, an original simulation of paste flow, Eur. J. Mech. A 15 (3) (1996) 465–485.

[10] G. Racineux, F. Chinesta, A. Poitou, Modélisation et identification du comportement rhéologique des pâtes minérales, 14$^{\text{ième}}$ Congrès Français de Mécanique, CDROM, Réf. 140, Toulouse, 1999, 6 pp.

[11] G. Dhatt, D.M. Gao, A.B. Cheikh, A finite element simulation of metal flow in molds, Int. J. Numer. Meth. Eng. 30 (1990) 821–831.

[12] M. Fortin, F. Brezzi, Mixed and Hybrid Finite Element Method, Springer, Berlin, 1991.

[13] R.W. Lewis, H.C. Huang, A.S. Usmani, J.T. Cross, Finite element analysis of heat transfer and flow problems using adaptive remeshing including application to solidification problems, Int. J. Numer. Meth. Eng. 32 (1991) 767–781.

[14] R.W. Lewis, A.S. Usmani, T.J. Cross, Efficient mold filling simulation in castings by an explicit finite element method, Int. J. Num. Meth. Fluids 20 (1995) 493–506.

[15] F. Ilinca, J.F. Hetu, A. Derdourai, Three dimensional modelling of metal powder injection molding, in: P. Martin, et al. (Eds.), MET SOC, Mathematical Modelling in Metals, Processing and Manufacturing, Ottawa, Ont., Canada, August 20–23, 2000, CDROM, pp. 1–14.